Vectorcardiographic diagnostic & prognostic information derived from the 12-lead electrocardiogram

Man, Sum-Che

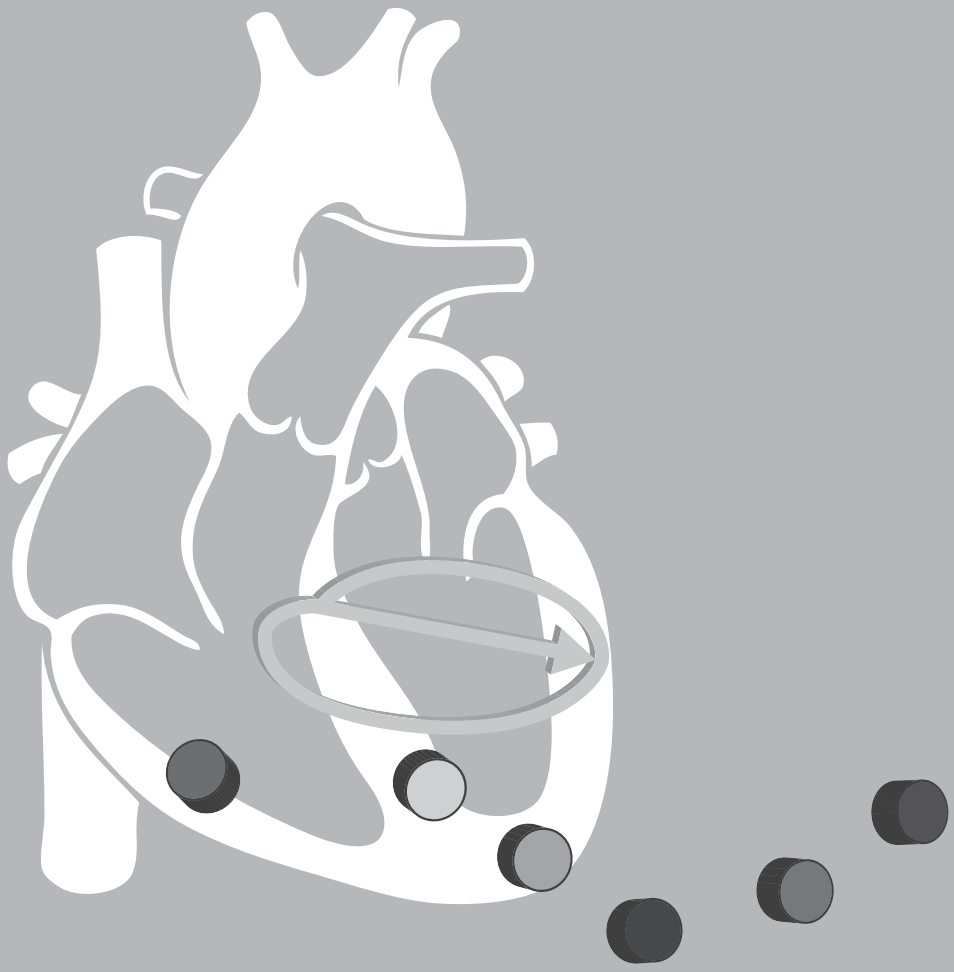

Chapter 6

The Spatial QRS-T Angle in the Frank VCG: Accuracy of Estimates Derived from the 12-Lead ECG

Charlotte A. Schreurs, Annemijn M. Algra, Sum-Che Man, Suzanne C. Cannegieter, Ernst E. van der Wall, Martin J. Schalij, Jan A. Kors, Cees A. Swenne

J Electrocardiol 2010; 43: 294-301

Abstract

Background

The spatial QRS-T angle (SA), a predictor of sudden cardiac death, is a vectorcardiographic variable. Gold standard vectorcardiograms (VCGs) are recorded by using the Frank electrode positions. However, with the commonly available 12-lead ECG, VCGs must be synthesized by matrix multiplication (inverse Dower matrix / Kors matrix). Alternatively, Rautharju proposed a method to calculate SA directly from the 12-lead ECG. Neither spatial angles computed by using the inverse Dower matrix (SA-D) nor by using the Kors matrix (SA-K) or by using Rautharju's method (SA-R) have been validated with regard to the spatial angles as directly measured in the Frank VCG (SA-F). Our present study aimed to perform this essential validation.

Methods

We analyzed SAs in 1220 simultaneously recorded 12-lead ECGs and VCGs, in all data, in SA-F-based tertiles, and after stratification according to pathology or sex.

Results

Linear regression of SA-K, SA-D and SA-R on SA-F yielded offsets of 0.01°, 20.3° and 28.3° and slopes of 0.96, 0.86 and 0.79, respectively. The bias of SA-K with respect to SA-F (mean ± SD –3.2 ± 13.9°) was significantly ($P < .001$) smaller than the bias of both SA-D and SA-R with respect to SA-F (8.0 ± 18.6° and 9.8 ± 24.6°, respectively); tertile analysis showed a much more homogeneous behavior of the bias in SA-K than of both the bias in SA-D and in SA-R. In pathologic ECGs, there was no significant bias in SA-K; bias in men and women did not differ.

Conclusion

SA-K resembled SA-F best. In general, when there is no specific reason to either synthesize VCGs with the inverse Dower matrix or to calculate the spatial QRST-angle with Rautaharju's method, it seems prudent to use the Kors matrix.

Introduction

The noninvasive identification of individuals at risk for life-threatening ventricular arrhythmias or sudden cardiac death presents a relevant clinical issue. The spatial QRS-T angle, a global ECG descriptor of cardiac repolarization and its relation to the preceding depolarization, is proven to be a variable with predictive value for sudden cardiac death. Several studies have shown that a wide spatial QRS-T angle, denoting a discordant ECG, is a predictor of sudden cardiac death: Kors *et al.* demonstrated this in an elderly population[1], Rautaharju *et al.* in a group of postmenopausal women[2], Kardys *et al.* in the general population[3] and Yamazaki *et al.*, Zhang *et al.* and De Torbal *et al.* in various clinical populations[4-6]. Furthermore, Borleffs *et al.* showed that a wide spatial QRS-T angle is also a strong predictor of appropriate device therapy in primary prevention implantable cardioverter defibrillator (ICD) recipients with ischemic heart disease[7].

The concept of the spatial QRS-T angle stems from vectorcardiography. However, nowadays, Frank vectorcardiograms (VCGs)[8] are usually not recorded in the clinic, and for spatial QRS-T angle calculation VCGs have to be synthesized from routine standard 12-lead ECGs.

Usually, VCG synthesis is done by multiplying the ECG by a conversion matrix. Most commonly, the inverse Dower matrix[9] or the Kors matrix[10] are used for this purpose. In addition, Rautaharju *et al.*[11] proposed a method to estimate the spatial QRS-T angle directly from a 12-lead ECG.

Interestingly, neither method to calculate the spatial QRS-T angle has been validated with respect to the gold standard, i.e. the spatial QRS-T angle measured in the Frank VCG. Therefore, the aim of our present study was to compare spatial QRS-T angles as computed in VCGs synthesized by the inverse Dower matrix and by the Kors matrix, as well as spatial QRS-T angles as computed by Rautaharju's method, to spatial QRS-T angles in original Frank VCGs.

Methods

Materials

We used data set #5 from the diagnostic library that was collected in the CSE (Common Standards for Quantitative Electrocardiography) project[12]. This data set consists of a clinical population of 1220 patients, each comprising a simultaneous 10s recording of the eight independent leads of the standard ECG (I, II, V1 to V6) and of the three Frank VCG leads X, Y, and Z. The sampling rate of the recordings is 500 Hz. Characteristics of the composition of CSE data #5 set in terms of sex, age, height and weight are known, however diagnostic statements are not provided with the data set, therefore, we used the diagnostic module of the ECG interpretation program MEANS[13] to separate the recordings into two categories: pathological (conduction disturbances, hypertrophy, infarction), or normal.

VCG synthesis

On the basis of the averaged P-QRS-T complexes, two synthesized VCG variants were calculated by multiplying the 12-lead ECGs by either the inverse Dower matrix or the Kors matrix. The inverse Dower matrix, introduced by Edenbrandt and Pahlm[9], is the pseudoinverse of the matrix proposed by Dower *et al.*[14], originally conceived for the purpose of 12-lead ECG synthesis from a VCG. This matrix is based on the Frank torso model and was created for simultaneous VCG and 12-lead ECG diagnostics in clinical Frank VCG recordings[14].

The second synthesized VCG variant was computed by using the ECG to VCG transformation matrix proposed by Kors and colleagues[10]. This matrix was based on a learning set from the CSE multi-lead library (data sets #3 and #4). It was generated by multiple linear regression, thus minimizing the root-mean-square differences between the synthesized VCG and the simultaneously recorded Frank VCG in a population of patients and normals. See Table 1 for the inverse Dower and Kors matrix coefficients. The spatial QRS-T angles were computed by MEANS. Subsequently, the spatial QRS-T angles were computed in the Frank VCGs and in the synthesized VCG variants.

TABLE 1. Coefficients of the inverse Dower and Kors ECG-to-VCG conversion matrices.

Inverse Dower Matrix	X	Y	Z	Kors Matrix	X	Y	Z
I	0.16	– 0.23	0.02	**I**	0.38	– 0.07	0.11
II	– 0.01	0.89	0.10	**II**	– 0.07	0.93	– 0.23
$\mathbf{V_1}$	– 0.17	0.06	– 0.23	$\mathbf{V_1}$	– 0.13	0.06	– 0.43
$\mathbf{V_2}$	– 0.07	– 0.02	– 0.31	$\mathbf{V_2}$	0.05	– 0.02	– 0.06
$\mathbf{V_3}$	0.12	– 0.11	– 0.25	$\mathbf{V_3}$	– 0.01	– 0.05	– 0.14
$\mathbf{V_4}$	0.23	– 0.02	– 0.06	$\mathbf{V_4}$	0.14	0.06	– 0.20
$\mathbf{V_5}$	0.24	0.04	0.06	$\mathbf{V_5}$	0.06	– 0.17	– 0.11
$\mathbf{V_6}$	0.19	0.05	0.11	$\mathbf{V_6}$	0.54	0.13	0.31

Rautaharju's method

The method proposed by Rautaharju *et al.*[11] for simplified assessment of the spatial QRS-T angle calculates the inverse cosine between approximations of the mean QRS and T vectors. This is a vectorcardiographically-based approach that, however, avoids full-blown VCG synthesis. Rautaharju *et al.* conclude that this simplified method can be seen as a satisfactory substitute for spatial QRS-T angles calculated from VCGs synthesized by the inverse Dower matrix. The X, Y and Z components of the mean QRS and T vectors are approximated by the net QRS and T amplitudes in the leads V5 (for QRS) or V6 (for T), aVF and V2, respectively. The spatial angle was computed from the MEANS measurement matrix as follows:

$$SA = ACOS[(QRSnet_{V6} * Tnet_{V5}) + (QRSnet_{aVF} * Tnet_{aVF}) + (QRSnet_{V2} * Tnet_{V2})] / (QRSsm * Tsm)$$

where

ACOS = inverse cosine,
QRSnet = R – abs(S or QS, whichever is larger),
Tnet = Tpos – abs(Tneg),
$QRSsm = SQRT[(QRSnet_{V6})^2 + (QRSnet_{aVF})^2 + (QRSnet_{V2})^2]$, and
$Tsm = SQRT[(Tnet_{V5})^2 + (Tnet_{aVF})^2 + (Tnet_{V2})^2]$.

In our study, the spatial QRS-T angles derived from Frank VCGs will be denoted as SA-F, the spatial angles computed in the VCGs synthesized by the inverse Dower matrix will be denoted as SA-D, the spatial angles computed in the VCGs

synthesized by the Kors matrix will be denoted as SA-K, and the spatial angles calculated by Rautaharju's method will be denoted as SA-R.

Statistical analysis

For visual comparison difference plots were made for SA-D, SA-K, and SA-R versus SA-F. To quantify bias we calculated the mean differences, their confidence intervals and P-values between either SA-D, SA-K or SA-R, and the gold standard, SA-F. To quantify noise we calculated the SD of the differences between either SA-D, SA-K or SA-R, and the gold standard, SA-F. Linear regression analysis was performed to further characterize the relation between SA-D and SA-F, between SA-K and SA-F, and between SA-R and SA-F. Similar analyses were performed after stratification into tertiles based on SA-F, to separately investigate the statistical behavior of the spatial angles for lower, middle and larger values. Also, separate analyses were done after stratification according to presence/absence of pathology and according to sex.

Results

CSE data set #5 comprises 1220 ECG/VCG recordings made in 831 caucasian men and 389 caucasian women. Mean ± SD age is 52±13 years. Height and weight are known in 1152 and 1150 cases, respectively; mean ± SD height is 169 ± 9 centimeters, mean ± SD weight is 71±12 kilograms.

Figure 1 shows two cases, with an acute and an obtuse spatial angle, respectively. The Figure depicts the scalar X-Y-Z leads, the vector loops and the QRS and T axes for the recorded Frank VCG and for the VCGs synthesized from the recorded 12-lead ECGs by the inverse Dower matrix and by the Kors matrix. A similar example of Rautaharju's method cannot be given as this method does not synthesize an actual VCG, but estimates the spatial QRS-T angle directly from the 12-lead ECG.

Table 2 shows the descriptive statistics of the 1220 spatial angles as derived from the Frank VCGs (SA-F), as derived from the VCGs synthesized by the inverse Dower (SA-D) and Kors (SA-K) matrices, and as calculated by Rautaharju's method

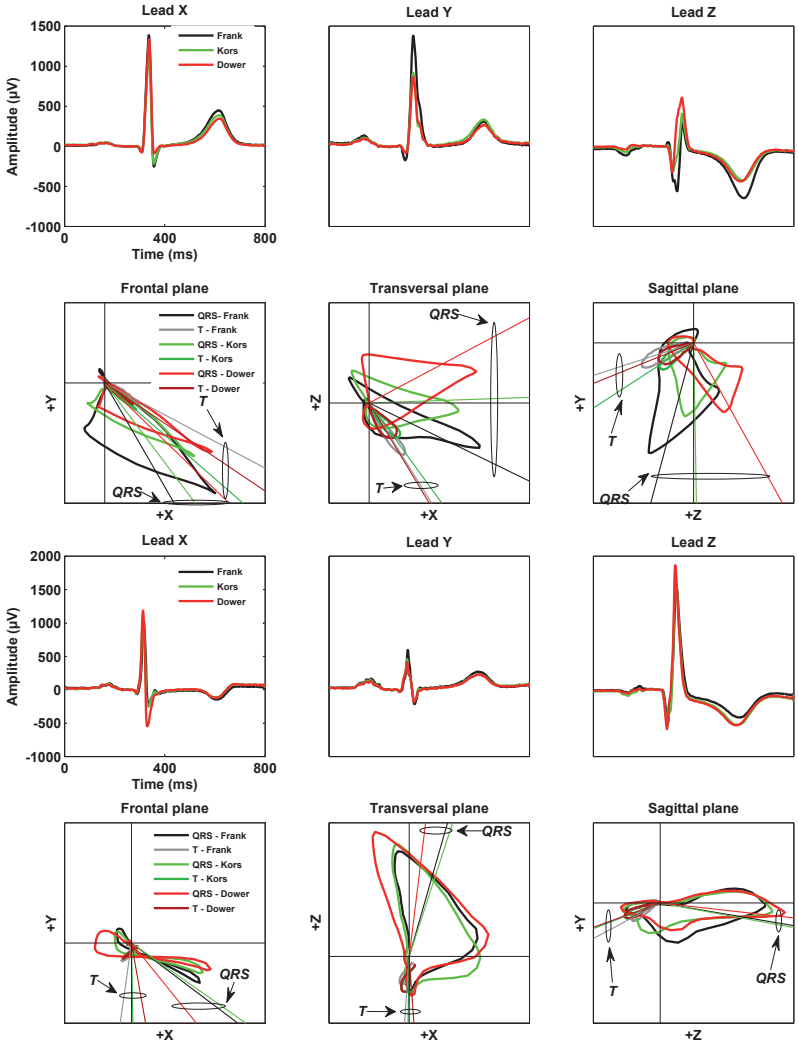

FIGURE 1. Superimposed Frank VCGs (black) and VCGs synthesized from the simultaneously recorded 12-lead ECG by multiplication by the inverse Dower matrix (red) and by the Kors matrix (green). Case A: subject in whom the Frank VCG has an acute spatial angle (48°). Case B: subject in whom the Frank VCG has an obtuse spatial angle (138°). The upper subplots depict the scalar X-Y-Z leads; the lower subplots depict the vector loops and the QRS and T axes in the frontal, transversal, and sagittal planes. The spatial angles cannot readily be observed in this figure as the frontal, transversal, and sagittal planes render the projections of the QRS and T axes. The figure demonstrates clearly that the scalar leads in subjects with relatively small spatial angles are predominantly concordant (in case A, all 3 leads X, Y, and Z are), whereas the scalar leads in subjects with relatively large spatial angles are predominantly discordant (in case B, leads X and Z are). In case A, the spatial angles of the synthesized VCGs are 48° (Kors matrix) and 76° (inverse Dower matrix), respectively. Obviously, the difference between the Dower VCG and the Frank VCG is quite dramatic here, especially when inspecting the vector loops. In case B, the spatial angles of the synthesized VCGs are 143° (Kors matrix) and 150° (inverse Dower matrix), respectively. In this case, the synthesized VCGs resemble the original Frank VCG much more.

(SA-R). SA-D (mean ± SD 95.3±39.0°) and SA-R (97.2±39.3°) were larger than SA-F (87.4±40.4°); in contrast, SA-K (84.1±41.3°) was smaller than mean SA-F.

TABLE 2. Descriptive statistics of the 1220 spatial QRS-T angles derived from the Frank VCGs (SA-F), derived from the VCGs synthesized by the inverse Dower (SA-D) and Kors (SA-K) matrices, and calculated by Rautaharju's method (SA-R).

CSE data set #5	Mean (95%CI) (°)	SD (°)	Median	(Interquartile range) (°)
SA-F	87.4 (85.1 to 89.6)	40.4	85	(55 to 117)
SA-D	95.3 (93.2 to 97.5)	39.0	93	(65 to 124)
SA-K	84.1 (81.8 to 86.4)	41.3	78	(51 to 115)
SA-R	97.2 (95.0 to 99.4)	39.3	96	(69 to 126)

Differences with the gold standard spatial angles measured in the Frank VCG, SA-F, are listed in Table 3. All mean differences differed significantly from zero, thus proving the existence of bias. Both bias (mean difference) and noise (SD of the differences) of SA-D with respect to SA-F (bias±noise is 8.0°±18.6°) and of SA-R with respect to SA-F (9.8°±24.6°) were considerably significantly larger ($P < .001$) than the bias and noise of SA-K with respect to SA-F (-3.2°±13.9°). The linear regression of SA-K on SA-F indicated a close correspondence between SA-K and SA-F (offset close to 0, slope close to 1, correlation close to 1). The linear regression of SA-D on SA-F yielded an offset of 20.34° and a slope of 0.86, indicating a lower degree of correspondence. The linear regression of SA-R on SA-F yielded an offset of 28.34° and a slope of 0.79, indicating an even lower degree of correspondence.

The agreement between SA-D and SA-F, between SA-K and SA-F, and between SA-R and SA-F is visualized in the three difference plots in Figure 2. As is readily appreciable in these plots, the distribution of the differences between SA-D and SA-F, and, the more so, the distribution of the differences between SA-R and SA-F, were wider than the distribution of the differences between SA-K and SA-F. Furthermore, the differences between SA-D and SA-F, and especially between SA-R and SA-F, seem to be less homogenously distributed than the differences between SA-K and SA-F. Therefore, tertile analysis was performed, which is shown in Table 3. Considerable differences in bias per tertile can be seen for both the comparisons of SA-D and SA-F and of SA-R and SA-F, in contrast to a much more homogenous behavior of the biases for the comparison of SA-K and SA-F over the full data range.

TABLE 3. Differences between SA-F (spatial QRS-T angles derived from Frank VCGs) and SA-D (spatial QRS-T angles derived from inverse-Dower-matrix synthesized VCGs), SA-K (spatial QRS-T angles derived from Kors-matrix-synthesized VCGs) and SA-R (spatial QRS-T angles calculated by Rautaharju's method), for all data, and for the subgroups that result after stratification according to SA-F tertiles, and according to sex or presence/absence of pathology.

	SA-F vs.	Mean difference (95%CI) (°)	P-value	SD of the differences (°)	Range of the differences (°)	Linear regression	*Correlation (r^2)*
All data (N = 1220)	**SA-D**	8.0 (7.0 to 9.0)	< .001	18.6	-70 to 73	D= 20.34 + 0.86F	0.79
	SA-K	-3.2 (-4.0 to -2.5)	< .001	13.9	-72 to 60	K= 0.01 + 0.96F	0.89
	SA-R	9.8 (8.4 to 11.2)	< .001	24.6	-113 to 141	R= 28.34 + 0.79F	0.66
TERTILES							
1st tertile 5° to 64° (N=406)	**SA-D**	13.5 (11.8 to 15.2)	< .001	17.5	-47 to 73	D= 17.71 + 0.90F	0.35
	SA-K	-1.1 (-2.2 to 0.1)	0.061	11.6	-44 to 60	K = 6.94 + 0.82F	0.51
	SA-R	18.8 (16.6 to 21.0)	< .001	22.5	-39 to 114	R= 22.43 + 0.92F	0.25
2nd tertile 65° to 103° (N=412)	**SA-D**	9.8 (7.9 to 11.6)	< .001	18.7	-42 to 68	D= 20.33 + 0.87F	0.23
	SA-K	-4.4 (-5.8 to -3.0)	< .001	14.5	-47 to 50	K= 1.60 + 0.93F	0.36
	SA-R	11.5 (9.2 to 13.8)	< .001	24.1	-72 to 78	R= 34.20 + 0.73F	0.11
3rd tertile 104° to 177° (N=402)	**SA-D**	0.6 (-1.1 to 2.3)	0.486	17.3	-70 to 43	D= 20.70 + 0.85F	0.51
	SA-K	-4.2 (-5.7 to -2.8)	< .001	15.2	-72 to 33	K= -5.25 + 1.01F	0.65
	SA-R	-0.9 (-3.2 to 1.3)	0.419	23.2	-141 to 67	R= 25.47 + 0.80F	0.34
SEX							
Men (N = 831)	**SA-D**	8.2 (6.9 to 9.5)	< .001	18.9	-60 to 73	D= 21.47 + 0.85F	0.78
	SA-K	-2.3 (-3.1 to -1.4)	< .001	12.9	-69 to 60	K= 2.54 + 0.95F	0.90
	SA-R	9.4 (7.7 to 11.1)	< .001	25.3	-141 to 114	R= 28.23 + 0.79F	0.64
Women (N = 389)	**SA-D**	7.6 (5.8 to 9.4)	< .001	18.0	-70 to 63	D= 18.24 + 0.87F	0.81
	SA-K	-5.3 (-6.9 to -3.7)	< .001	15.7	-72 to 50	K= -4.64 + 0.99F	0.87
	SA-R	10.7 (8.4 to 13.1)	< .001	23.2	-81 to 80	R= 28.51 + 0.79F	0.69
PATHOLOGY							
Normal (N = 640)	**SA-D**	10.3 (9.1 to 11.6)	< .001	16.4	-57 to 73	D= 20.47 + 0.86F	0.78
	SA-K	-5.7 (-6.7 to -4.7)	< .001	12.9	-48 to 48	K= -0.51 + 0.93F	0.87
	SA-R	12.0 (10.3 to 13.7)	< .001	22.0	-81 to 80	R= 28.82 + 0.77L	0.63
Pathological (N = 580)	**SA-D**	5.4 (3.7 to 7.1)	< .001	20.5	-70 to 68	D= 19.46 + 0.86F	0.76
	SA-K	-0.5 (-1.7 to 0.7)	0.425	14.5	-72 to 60	K= 6.65 + 0.93F	0.88
	SA-R	7.4 (5.2 to 9.6)	< .001	27.0	-141 to 114	R= 29.41 + 0.79F	0.61

In the subgroup-analyses there were no significant differences between males and females (Table 3). With respect to pathology, differences of SA-F stratified into spatial angles from pathological ECGs (n = 580) and spatial angles from normal ECGs (n = 640) are given in Table 3. Bias, noise and the regression equation for SA-K on SA-F were superior to both that of SA-D on SA-F and SA-R on SA-F, respectively,

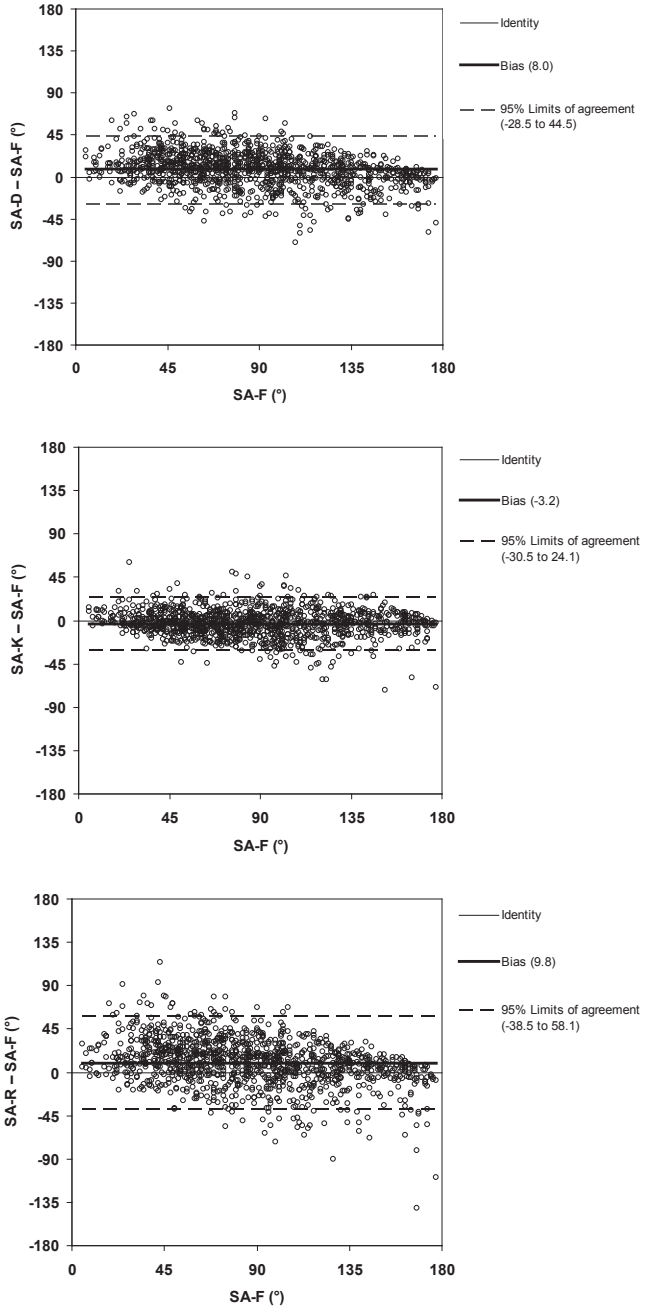

FIGURE 2. Difference plots for (upper panel) the spatial QRS-T angles computed in the inverse Dower matrix synthesized VCG (SA-D) and in the Frank VCG (SA-F), for (middle panel) the spatial QRS-T angles computed in the Kors-matrix synthesized VCG (SA-K) and in the Frank VCG (SA-F), and for (lower panel) the spatial QRS-T angles calculated by Rautaharju's method (SA-R) and computed in the Frank VCG (SA-F).

especially in the pathological category. As expected, the SA-F for the pathologic cases (mean ± SD 102.8°±40.7) were significantly larger (mean ± SD difference is 29.8°±54.2; 95% CI 34.2° to 25.4°) than for the normal ECGs (mean ± SD, 73.0° ± 34.8°).

Discussion

We compared, in simultaneously recorded 12-lead ECGs and VCGs, the spatial QRS-T angles derived from two synthesized VCG variants, using the inverse Dower matrix[9] and the Kors matrix[10], as well as the spatial QRS-T angles calculated by Rautaharju's method[11], to the spatial QRS-T angles derived from original Frank VCGs. Taking SA-F as gold standard, we found that the correspondence of the spatial QRS-T angles computed on the basis of the VCGs synthesized with the Kors matrix was superior in terms of bias and noise (mean and spread of the differences), and also in terms of the linear regression over the full range of the angles (Table 3).

As can be seen in the tertile analysis (table 3), the Kors matrix behaved constantly well for all spatial QRS-T angle magnitudes, showing a more homogenous behavior in comparison to the spatial QRS-T angles computed by the inverse Dower matrix and by Rautaharju's method, which both had hardly any bias in the third tertile, in contrast to a much larger bias present in the first and second tertile. However, when looking at slope and correlation in the third tertile, it is the Kors matrix that performs best, creating a more balanced picture. Furthermore, as can be observed in the analysis after stratification into normal and pathological ECGs (table 3), the Kors matrix performs better than the inverse Dower matrix and Rautaharju's method in both normal and pathological ECGs, for each measure of correspondence that we used.

In the normal human heart, the repolarization wavefront does not follow the preceding depolarization wave front, because action potentials in cardiac regions that are depolarized last tend to be briefer than action potentials in regions of the heart that are activated first[15]. This causes the heart vector to grossly assume the same direction during the QRS complex and the T wave, which manifests in the form of a concordant ECG (equal polarity of the QRS complex and the T wave in

most ECG leads). In the diseased heart this property is partially lost, which causes the QRS and T axes to deviate more in direction, manifesting as discordance in the ECG. Hence, the spatial angle between the QRS and the T axes is expected to be relatively acute in normal ECGs and relatively obtuse in pathological ECGs. However, a normal ECG can have a larger spatial QRS-T angle, while a pathological ECG can have a smaller spatial QRS-T angle, creating a substantial overlap. When determining the accuracy of the spatial QRS-T angle, it would give a one-sided view to only look at the larger angles. Therefore, it is important that the behavior of the spatial angles after stratification into normal and pathological ECGs is also taken into consideration.

Alternative measurements

In addition to the "real" QRS-T spatial angle, which is defined as the angle between the QRS and T axes, several alternatives have been proposed, sometimes because of presumed simplicity of calculus, sometimes because of potential improvement in terms of physiological interpretation or predictive value.

Malik *et al.* proposed to calculate the "total cosine R-to-T" (TCRT)[16] between the QRS and T vectors in a mathematically reconstructed 3-D space, consisting of the principal three dimensions after singular value decomposition of the ECG. Although this angle also has predictive power[16], it cannot be compared with the spatial QRS-T angles in the VCG, because TCRT angles are defined in signal space rather than in VCG image space. Even though there is sometimes good correspondence between the 3-D spaces after singular value decomposition and the VCG image space, this is not an intrinsic property of the principal component analysis methodology that underlies the singular-value decomposed ECG.

Zhang[5] and Pavri *et al.*[17] demonstrated that also the planar QRS-T angle is a significant predictor of sudden cardiac death. Obviously, the planar QRS-T angle (the projection of the spatial QRS-T angle on the frontal plane) can differ dramatically from the spatial QRS-T angle, depending on the orientation of the QRS and T axes. The advantage of the planar over the spatial QRS-T angle would be that it can be assessed in the standard 12-lead ECG by simple visual inspection. Again, it is questionable whether this calculus is simpler than the straightforward calculation

in the VCG, while the original 3D concept, that is invariant for, *e.g.*, anatomical rotations between subjects, is sacrificed.

Dilaveris and colleagues have published remarkably small spatial QRS-T angles: a study on normal subjects gave a mean spatial angle of 20.4°[18]. Other studies from this same group, amongst others on the effects of cigarette smoking[19], high blood pressure[20] and on myocardial infarction survivors[21], all presented small spatial angles, as did a study by Jaroszynski *et al.*[22], who used the same analysis method. Dilaveris and colleagues consistently use the inverse Dower matrix to reconstruct the VCG from an average beat computed by the MEANS program[13], after which the spatial QRS-T angles are calculated according to locally developed dedicated software. Prompted by these striking differences we have additionally verified the reliability of the spatial angles as calculated by MEANS. This was done by comparing the spatial angles as calculated by the LEADS program[23] in the study by Scherptong *et al.*[24] by the spatial angles computed by the MEANS program in the same data set. The LEADS program has been developed in the Leiden University Medical Center independently from MEANS and is interactive in the sense that onset and offset of QRS and T are manually verified (while this is an automated procedure in MEANS). A mean difference of 1.9° (SD 3.7, 95% CI 1.6 to 2.2) was found. However, this difference is that small and there is such a good linear relationship ($SA_{LEADS}=0.52 + 1.02SA_{MEANS}$, $R^2=0.99$), that this makes us confident that the spatial angle calculus in MEANS is correct. In our view, the deviating angles mentioned above can only be explained by a different calculus that we regrettably cannot further specify on the basis of the Methods sections in these publications.

Normal limits

The results of our current study demonstrate that the spatial QRS-T angle in a given subject depends strongly on the origin of the VCG (Frank, or synthesized with the inverse Dower or Kors matrix) or calculus (Rautaharju's method). Hence, when making use of normal limits for spatial angles for diagnostic/prognostic purposes, one must use normal limits fit for the specific spatial angle. Thus, better diagnostic performance of the spatial angle can be expected.

Normal limits for the QRS-T spatial angle have been defined in a few studies. Pipberger and colleagues were the first to publish normal limits of the spatial

angle from 8-electrode 3-lead Frank VCGs recorded in 518 hospitalized men[25;26]. The normal limits for spatial angles presented by Pipberger and associates were 26° to 134°. Although this study population was without cardiovascular disease, it is questionable if such a group can be regarded as healthy, because noncardiac disease and the administration of noncardiac medication could still have induced changes in cardiac electrophysiology resulting in (temporary) changes of the spatial QRS-T angle. However, for long, this has been the only source for normal limits of the spatial angle: studies by Kors et al, Kardys et al, and De Torbal et al, while calculating spatial angles from Kors matrix synthesized VCGs, all used 135° as the threshold for abnormal angles.

Recently, Scherptong *et al.* determined normal limits of the spatial QRS-T angle, as derived from VCGs synthesized by the inverse Dower matrix. As database they used 660 healthy male and female medical students[24]. Normal limits appeared to be different for males (30° to 130°) and for females (20° to 116°), hence they concluded that sex should be taken into account when using the spatial QRS-T angle for risk analysis.

Obviously, when QRS-T spatial angles of a given population are to be contrasted with normal values, such normal values ought to be determined in an appropriate group (*e.g.*, healthy persons of matching age and sex) and in an appropriate way (i.e., using similar ECG recording and processing techniques). As our study demonstrates, there is quite a good agreement, in terms of bias, between the spatial angles measured in a Frank VCG and measured in a VCG that was synthesized from a 12-lead ECG by using the Kors matrix[10]. However, there is a considerable amount of noise, which has an impact on the normal values. Bias and noise are even larger in SAs computed in VCGs synthesized by the inverse Dower matrix and in SAs computed by direct calculation from the ECG according to Rautaharju and coworkers[11]. Summarizing, a new set of Frank VCG measurements in normal subjects is needed to reestablish or refine the existing normal values that were published by the group of Pipberger and colleagues[25;26]. Moreover, and in addition to the normal values as calculated in inverse-Dower-synthesized VCGs[24], normal values should be calculated in a set of Kors-matrix-synthesized normal VCGs.

Because in some clinical situations the 10 electrodes needed for the standard 12-lead ECG are impractical, there is upcoming interest in reduced lead sets and in the synthesis of 12-lead ECGs and of VCGs on the basis of these lead sets[27;28]. Our study focused on the widespread 10-electrode configuration of the standard 12-lead ECG, but it might be important to study the accuracy of spatial QRS-T angles derived from VCGs synthesized from reduced lead sets as well.

Limitations

The validated diagnoses of the CSE diagnostic library remain under lock and key in the CSE coordinating center. Hence, when stratifying the data set according to presence/absence of pathology we had to rely on the MEANS diagnostic module when classifying the ECGs as normal or as associated with bundle branch block, hypertrophy and infarction. We cannot exclude that the MEANS diagnostic module missed repolarization abnormalities.

Conclusions

In our study, spatial QRS-T angles that were calculated using the Kors VCG synthesizing matrix showed superior correspondence with the spatial QRS-T angles in the original Frank VCGs in comparison with the spatial QRS-T angles from the VCG synthesized by the inverse Dower matrix and even more in comparison to the spatial QRS-T angles calculated by Rautaharju's method. Moreover, the Kors matrix supplies better resembling spatial QRS-T angles for each angle magnitude, in contrast to both the inverse Dower matrix and Rautaharju's method. In general, when there is no specific reason to either synthesize VCGs with the inverse Dower matrix or to calculate the spatial QRST-angle with Rautaharju's method, it seems prudent to use the Kors matrix.

References

1. Kors JA, Kardys I, Van der Meer I, Van Herpen G, Hofman A, Van der Kuip DA, Witteman JC. Spatial QRS-T angle as a risk indicator of cardiac death in an elderly population. *J Electrocardiol* 2003;36 Suppl:113.
2. Rautaharju PM, Kooperberg C, Larson JC, LaCroix A. Electrocardiographic abnormalities that predict coronary heart disease events and mortality in postmenopausal women: the Women's Health Initiative. *Circulation* 2006;113:473.
3. Kardys I, Kors JA, Van der Meer I, Hofman A, Van der Kuip DA, Witteman JC. Spatial QRS-T angle predicts cardiac death in a general population. *Eur Heart J* 2003;24:1357.
4. Yamazaki T, Froelicher VF, Myers J, Chun S, Wang P. Spatial QRS-T angle predicts cardiac death in a clinical population. *Heart Rhythm* 2005;2:73.
5. Zhang ZM, Prineas RJ, Case D, Soliman EZ, Rautaharju PM. Comparison of the prognostic significance of the electrocardiographic QRS/T angles in predicting incident coronary heart disease and total mortality (from the atherosclerosis risk in communities study). *Am J Cardiol* 2007;100:844.
6. De Torbal A, Kors JA, Van Herpen G, Meij S, Nelwan S, Simoons ML, Boersma E. The electrical T-axis and the spatial QRS-T angle are independent predictors of long-term mortality in patients admitted with acute ischemic chest pain. *Cardiology* 2004;101:199.
7. Borleffs CJ, Scherptong RW, Man SC, Van Welsenes GH, Bax JJ, Van Erven L, Swenne CA, Schalij MJ. Predicting ventricular arrhythmias in patients with ischemic heart disease: clinical application of the ECG-derived QRS-T angle. *Circ Arrhythm Electrophysiol* 2009;2:548.
8. Frank E. An accurate, clinically practical system for spatial vectorcardiography. *Circulation* 1956;13:737.
9. Edenbrandt L and Pahlm O. Vectorcardiogram synthesized from a 12-lead ECG: superiority of the inverse Dower matrix. *J Electrocardiol* 1988;21:361.
10. Kors JA, Van Herpen G, Sittig AC, Van Bemmel JH. Reconstruction of the Frank vectorcardiogram from standard electrocardiographic leads: diagnostic comparison of different methods. *Eur Heart J* 1990;11:1083.
11. Rautaharju PM, Prineas RJ, Zhang ZM. A simple procedure for estimation of the spatial QRS/T angle from the standard 12-lead electrocardiogram. *J Electrocardiol* 2007;40:300.
12. Willems JL, Abreu-Lima C, Arnaud P, Van Bemmel JH, Brohet C, Degani R, Denis B, Gehring J, Graham I, van HG, . The diagnostic performance of computer programs for the interpretation of electrocardiograms. *N Engl J Med* 1991;325:1767.
13. Van Bemmel JH, Kors JA, Van Herpen G. Methodology of the modular ECG analysis system MEANS. *Methods Inf Med* 1990;29:346.
14. Dower GE, Machado HB, Osborne JA. On deriving the electrocardiogram from vectoradiographic leads. *Clin Cardiol* 1980;3:87.
15. Jeyaraj D, Wilson LD, Zhong J, Flask C, Saffitz JE, Deschenes I, Yu X, Rosenbaum DS. Mechanoelectrical feedback as novel mechanism of cardiac electrical remodeling. *Circulation* 2007;115:3145.

16. Malik M, Hnatkova K, Batchvarov VN. Post infarction risk stratification using the 3-D angle between QRS complex and T-wave vectors. *J Electrocardiol* 2004;37 Suppl:201.
17. Pavri BB, Hillis MB, Subacius H, Brumberg GE, Schaechter A, Levine JH, Kadish A. Prognostic value and temporal behavior of the planar QRS-T angle in patients with nonischemic cardiomyopathy. *Circulation* 2008;117:3181.
18. Dilaveris P, Pantazis A, Gialafos E, Triposkiadis F, Gialafos J. Determinants of electrocardiographic and spatial vectorcardiographic descriptors of ventricular repolarization in normal subjects. *Am J Cardiol* 2001;88:912.
19. Dilaveris P, Pantazis A, Gialafos E, Triposkiadis F, Gialafos J. The effects of cigarette smoking on the heterogeneity of ventricular repolarization. *Am Heart J* 2001;142:833.
20. Dilaveris P, Gialafos E, Pantazis A, Synetos A, Triposkiadis F, Gialafos J. The spatial QRS-T angle as a marker of ventricular repolarisation in hypertension. *J Hum Hypertens* 2001;15:63.
21. Giannopoulos G, Dilaveris P, Batchvarov V, Synetos A, Hnatkova K, Gatzoulis K, Malik M, Stefanadis C. Prognostic significance of inverse spatial QRS-T angle circadian pattern in myocardial infarction survivors. *J Electrocardiol* 2009;42:79.
22. Jaroszynski A, Czekajska-Chechab E, Drelich-Zbroja A, Zapolski T, Ksiazek A. Spatial QRS-T angle in peritoneal dialysis patients: association with carotid artery atherosclerosis, coronary artery calcification and troponin T. *Nephrol Dial Transplant* 2009;24:1003.
23. Draisma H.H.M., Swenne, C. A., Van de Vooren H., and *et al.* LEADS: an interactive research oriented ECG/VCG analysis system. *Comput in Cardiol* 2005;32:515.
24. Scherptong RW, Henkens IR, Man SC, Le Cessie S, Vliegen HW, Draisma HH, Maan AC, Schalij MJ, Swenne CA. Normal limits of the spatial QRS-T angle and ventricular gradient in 12-lead electrocardiograms of young adults: dependence on sex and heart rate. *J Electrocardiol* 2008;41:648.
25. Draper HW, Peffer CJ, Stallmann FW, Littmann D, Pipberger HV. The corrected orthogonal electrocardiogram and vectorcardiogram in 510 normal men (Frank lead system). *Circulation* 1964;30:853.
26. Pipberger HV, Goldman MJ, Littmann D, Murphy GP, Cosma J, Snyder JR. Correlations of the orthogonal electrocardiogram and vectorcardiogram with consitutional variables in 518 normal men. *Circulation* 1967;35:536.
27. Feild DQ, Feldman CL, Horacek BM. Improved EASI coefficients: their derivation, values, and performance. *J Electrocardiol* 2002;35 Suppl:23.
28. Horacek BM, Warren JW, Wang JJ. On designing and testing transformations for derivation of standard 12-lead/18-lead electrocardiograms and vectorcardiograms from reduced sets of predictor leads. *J Electrocardiol* 2008;41:220.